



ISSN: 0067-2904

Imaging through turbid medium utilizing spatial light modulator

H. A. Naser^{1*}, K. A. Al-Naimee^{1,2}

¹Department of Physics, College of Science, University of Baghdad, Baghdad, Iraq

²Istituto Nazionale di Ottica - CNR, Largo E. Fermi 6, 50125 Florence, Italy

Abstract:

The spatial light modulator (SLM) is utilized to compensate wave front aberrations due to a highly scattering medium. A He-Ne laser is transmitted through a turbid medium and produced a random speckle pattern, the intensity of one of the speckles can be easily enhanced by applying the appropriate SLM phase pattern. A bright spot with a contrast proportional to the number of controlled SLM segments appears on the screen. The images captured with the CCD camera before and after the optimization.

Keywords: spatial light modulator, turbid medium, wavefront correction.

التصوير خلال الوسط المضطرب باستخدام المضمن المكاني الضوئي

حيدر عايد ناصر^{1*}، قيس عبد الستار النعيمي^{1,2}

¹قسم الفيزياء، كلية العلوم، جامعة بغداد، بغداد، العراق

²المركز الوطني للبصريات، لاركو انريكو فيرمي، فلورنس، ايطاليا

الخلاصة:

تم استخدام مضمن الضوء المكاني (SLM) لتصحيح زيوغ جبهة الموجه الساقطة الناتج من الاستطارة العالية للوسط المضطرب. عند نفوذ ليزر الهيليوم نيون خلال الجسم المضطرب تم الحصول على طراز الرقطة العشوائي، تم تحسين شدة تلك الرقطة باستخدام جهاز (SLM). تم الحصول على بقعة مضئية تتناسب شدتها مع قدرة تحليل الجهاز المستخدم، وتم تسجيل النتائج باستخدام كاميرا قبل وبعد التصحيح.

I. Introduction

Examine diffuse light in the high scattering regime has become a very functioning field of research [1]. First, the attention was in investigative characteristics of photon diffusion in turbid biological media [2].

In recent years, high resolution wavefront shaping has developed as a dominant approach to generate a pointed focus through such as materials [3]. Optical signal transmission through random media has many applications, including deep-tissue imaging [4], underwater navigation, in early cancer detection, dynamic spectroscopy techniques, and atmospheric sensing or telecommunications [5-8].

In many random photonic materials (such as paper, paint and tissue) light is multiply scattered. As a result, the propagation of light becomes diffuse and the materials appear to be opaque [9-11], in these materials, repeated scattering and interference distort the incident wavefront so strongly that all spatial coherence is lost [12-13]. So incident coherent light diffuses through the random medium and forms a volume speckle field that has no correlations on a distance larger than the wavelength of light [11, 14, 15]. However, the obtaining of an image of structures embedded within or behind turbid media and enhanced spatial resolution has remained to be one of the most challenging problems in the fields of physics, biology, and medical diagnostics [16]. The high amount of light scattering in such

*Email: haider.ayedgggg@gmail.com

media tends to blur the projections of light through the medium represent the main problem [17]. Wavefront shaping using a spatial light modulator (SLM) with a surprisingly small number of degrees of control (as compared to the number of scattered modes, i.e., speckles) represents the solve of this problem [12].

Holography can be used to produce an undistorted image of an object which is located behind a distorting medium [18]. Correcting the optical aberration with a SLM will focus the light to a nearly ideal point and also make the computer generated hologram (CGH) sharper and clearer. The SLM achieves high precision and high efficiency laser machining by correcting optical aberration in the turbid medium [19]. SLMs are very useful devices due to their intrinsic gray scale ability [20].

The SLMs are used to compensate dynamic wavefront aberrations [19,21]. Resolution is another important characteristic of SLMs; it affects the uncorrected aberration left after applying the SLM correction due to the discrete structure of the optical path difference (OPD) introduced by the SLM. The correction is done in real-time by continuously sensing the incoming wavefront and adjusting the OPD of an SLM to compensate aberrations [22]. Wavefront correction allows forming a nearly optimal focus inside a turbid sample [7, 23]. In this work, a technique based on high-resolution wavefront shaping that enables real-time wide-field imaging in three dimensions using diffuse scattered light was presented.

II. Dynamical model

When polarizing light is incident on SLM it will be modulate due to pixelated liquid crystals, so the output intensity will dependent on the driving voltage of SLM [24-27].

A disordered speckle pattern is recorded by placing a disordered medium, so the transmitted wave is lost all correlation with the incident wavefront because of scattered and diffracted light about a hundred times [28], which will prevent the wavefront correction by adaptive optics [29]. The correlation can be restored by shaping the wavefront of the incident light using a SLM [30, 31]. Consider N is the order of the nonlinearity, and N_{speckles} is the number of speckle obtained by putting a scattering medium in the path of incident wave. Assuming that the incident beam is scattered to a number of speckles N_{speckles} on a simple nonlinear object. The generated power would be proportional to [3]:

$$P_{\text{tot}} \propto N_{\text{speckles}} \cdot \left(\frac{P_{\text{laser}}}{N_{\text{speckles}}} \right)^N = P_{\text{laser}}^N \left(\frac{1}{N_{\text{speckles}}} \right)^{N-1} \quad (1)$$

Where P_{laser} is the power of incident laser beam on the turbid medium. From equation (1), when $N > 1$, the generated power would maximize for a beam where N_{speckles} is minimized, i.e. most focused beam. Consider a Gaussian beam focused to a waist ω_0 inside turbid medium, an N^{th} -order nonlinear signal will produce. The measured nonlinear signal can be approximated by the signal generated inside a cylinder of volume V along the beam confocal parameter $b = 4\pi\omega_0^2/\lambda$. The measured signal would be proportional to: [3]

$$P_{\text{tot}} \propto V \cdot I_{\text{laser}}^N \propto (b \cdot \pi \omega_0^2) \cdot \left(\frac{P_{\text{laser}}}{\omega_0^2} \right)^N \propto \omega_0^4 \cdot \left(\frac{P_{\text{laser}}}{\omega_0^2} \right)^N \propto \frac{P_{\text{laser}}^N}{\omega_0^{2(N-2)}} \quad (2)$$

From equation (2), the measured signal is constant (independent of ω_0) for $N = 2$. So, correction in an opaque, second-order medium is not possible. Only for $N > 2$, (i.e., only for a nonlinearity), the obtained signal increase due to focus. If the resolution is too low, the uncorrected aberration will affect the image quality [22-23].

III. Experimental Results

The SLM of Holoeye LC2002 model is used with resolution of 800×600 pixels ($32 \mu\text{m}$ square in size) and 256 grey level signal display. The power of SLM up to 2W without any external cooling. Figure-1 shows a schematic diagram of the optical layout by using HeNe-laser of 632.8nm wavelength. In this optical system without disorder, the sharpness of the focus is limited by the numerical aperture and the quality of the lens.

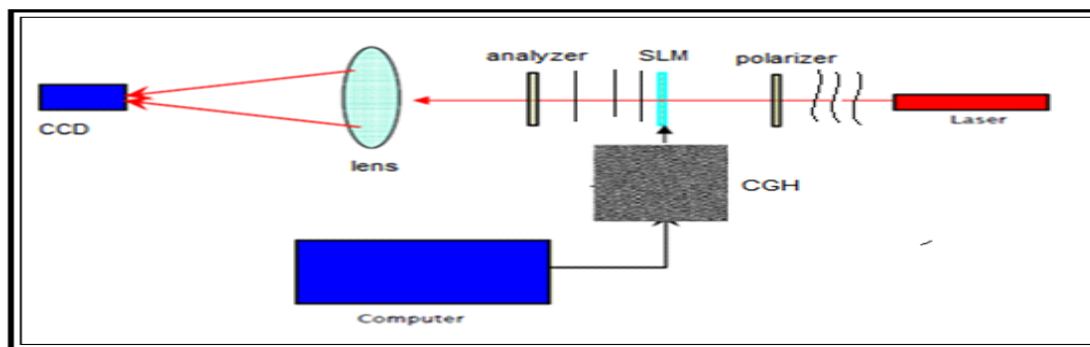


Figure 1- Experimental setup of wavefront correction using SLM, a polarizer is used to create linearly polarized light. Using a second polarizer as an analyzer. A programmable SLM will rotate the polarization. The amount of rotation is regulated by applying a voltage over the SLM. A lens focuses a beam of light onto a charge coupled device (CCD) camera.

The pattern of He-Ne laser which incident on CCD camera is shown in Figure-2.

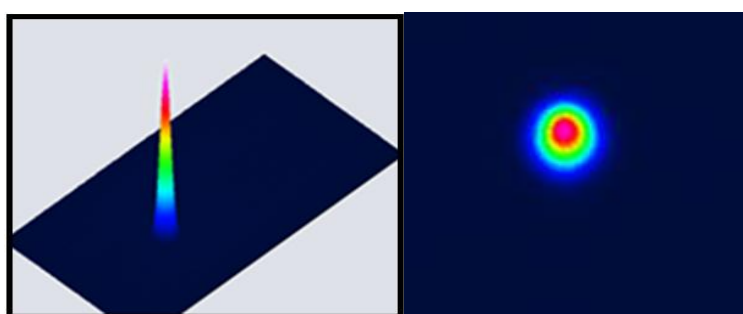


Figure 2- The intensity profile of the He-Ne laser pulse (a) 3D, and (b) 2D display.

The images captured with the CCD camera before the optimization is shown in Figure-3. The effect of putting a diffuser in front of the laser source is random speckles, Figure-3b. After using the SLM, the transmitted intensity pattern is ordered by a single bright spot in the screen, Figure-4.

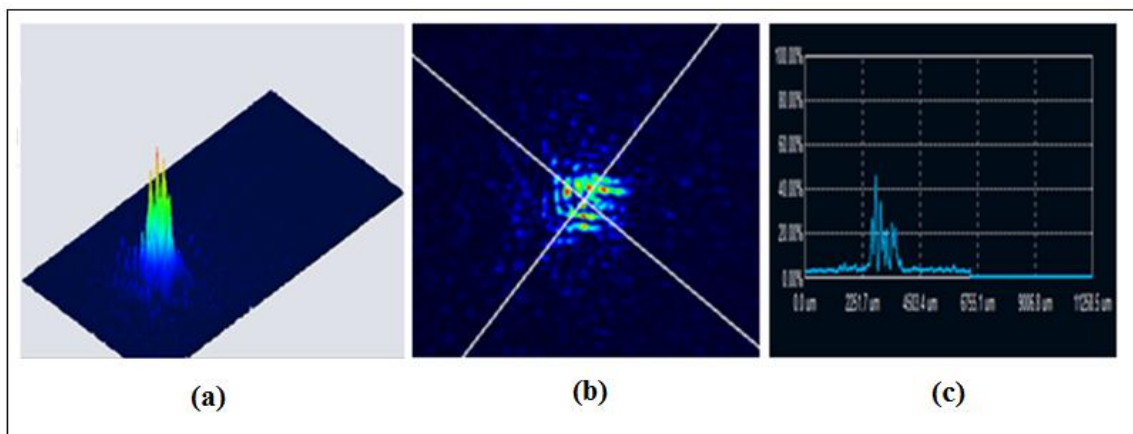


Figure 3-Experimental results of the optimizationsystem. (a) 3D display of the disturbed HeNe laserbeam before optimization (b) 2D display of the HeNe laser before optimizationshows the speckle, spatially scattered recorded from the CCD (c) XY scale of intensity distribution of HeNe laser before optimization.

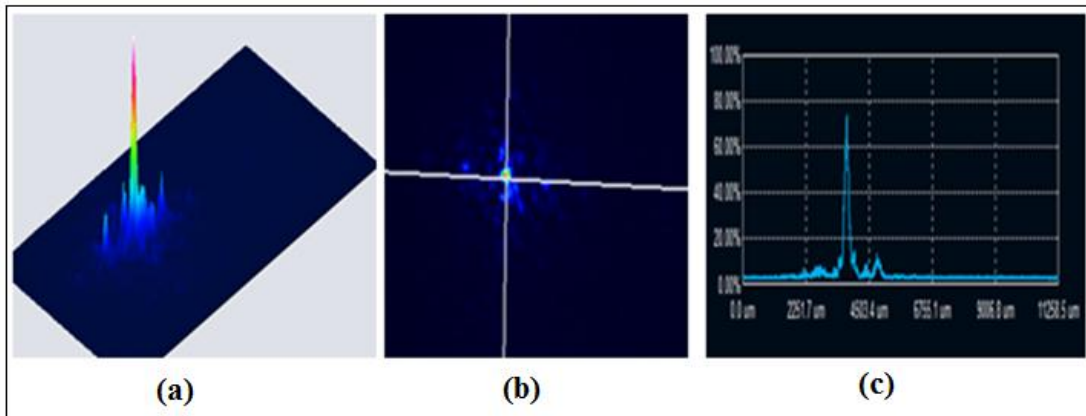


Figure 4- Experimental results of the optimization system for HeNe laser beam after using SLM. (a) 3D display of HeNe laser beam after optimization (b) 2D display of the HeNe laser after optimization (c) XY scale of intensity distribution of HeNe laser after optimization

Linearly polarized light from a He–Ne laser is expanded by a diffractive lens, Figure-5, and then transmitted through the SLM. When the polarization of the illuminating light is oriented along the extraordinary axis of the liquid crystal (LC) cells, the SLM will be act as a phase modulator.

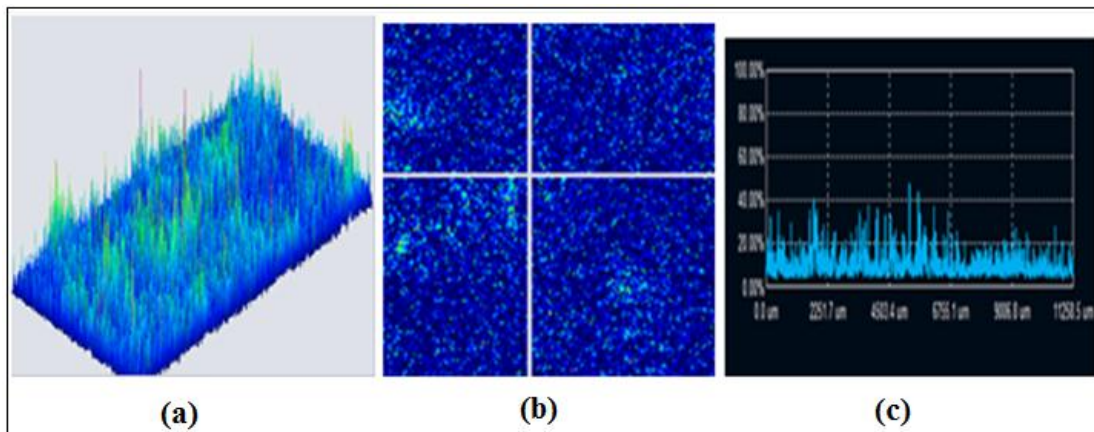


Figure 5- Experimental results of the optimization system for expand HeNe laser beam. (a) 3D display of the disturbed HeNe laser beam before optimization (b) 2D display of the HeNe laser before optimization (c) XY scale of intensity distribution of HeNe laser before optimization.

After optimization, Figure-6, the optical correction and the distortion compensation due to the effect of the SLM is clear.

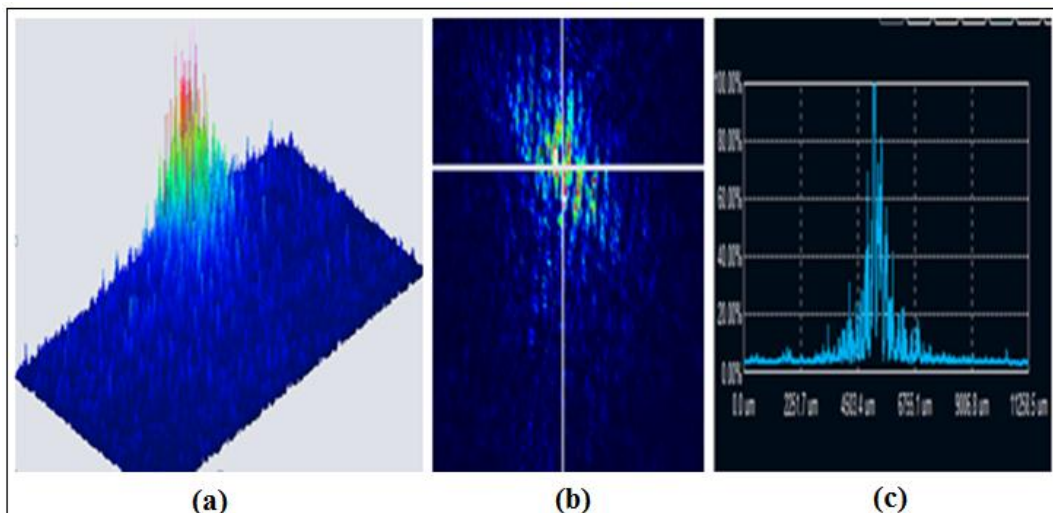


Figure 6- Experimental results of the optimization system for expand HeNe laser beam after using SLM. (a) 3D display of HeNe laser beam after optimization (b) 2D display of the HeNe laser after optimization (c) XY scale of intensity distribution of HeNe laser after optimization.

In order to test visual acuity, a pinhole is applied as an alternative to corrective lenses, as shown in Figure-7 to focus light and to low-pass filter the Fourier plane of the SLM, so the maximum improvement in results could be achieved.

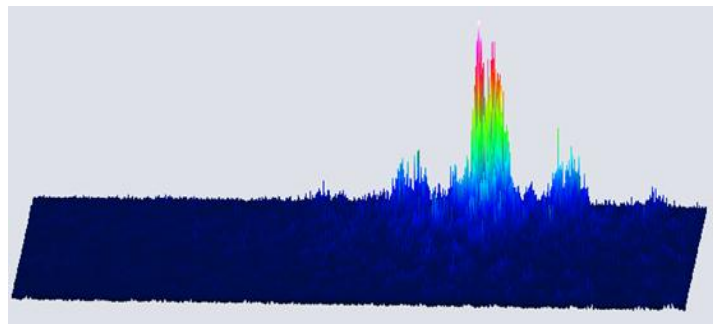


Figure 7- 3D display, the face of the SLM was imaged onto a camera through a pinhole that passed only the first diffraction orders produced by the SLM.

IV. Results and Discussion:

The surface area of the SLM is subdivided into 800×600 pixels, which are phase-modulated. The surface of the SLM is imaged onto the central plane of the lens. The optimal wavefront is completely disordered, which verifies that the sample is intensely scattering. The true image of the laser, with the diffuser removed, is shown in Figure-2. The point source produces a random speckle pattern on the camera due to highly scattering medium Figures-3b, 5b.

Figure-4 shows the intensity distribution after running the SLM. The surface of the scattering medium is imaged to the plane of a two-dimensional SLM. The dispersed light focuses to a fitted spot then focused onto a CCD camera by a lens with focal length $f=10\text{cm}$. even though the SLM did not optimize the shape of the focus obviously, dispersion has greatly recovered the focusing resolution. The unshaped parts of the beam would also display some amplitude modulation. On the camera, this caused variations in intensity over a much larger region of the beam.

The image that was obtained with the optimized focus Figure-4 and Figure-6 is of higher resolution and contrast and approximately brighter than an image obtained without optimization Figure-3 and Figure-5 because of using the SLM. The rise in intensity is probably caused by a natural birefringence of the SLM. The parallel polarization will then always be given a phase delay compared to the orthogonal polarization. Initially, an applied phase delay will compensate this refractive index difference and cause the intensity to rise.

Conclusion

In conclusion, a new technique to study the correction of distortion wavefront due to a highly scattered medium utilizing SLM is presented. This technique demonstrates that SLM can be successfully focused behind a highly dispersal medium, and corrected the aberration distortion on the CCD. The dynamical model describes this mechanism is demonstrated.

The diffraction performance of the SLM at HeNe laser beam of 632.8nm wavelength is evaluated. The random speckles caused by scattering medium is captured by using CCD camera, the effects of SLM before and after optimization is studied.

Acknowledgment

The authors would like to thank R.Meucciati INO-CNR for his precious scientific debate.

References:

1. R. Pierrat, N. B. Braham, L.F. Rojas-Ochoa, R. Carminati and F. Scheffold. **2008**. The influence of the scattering anisotropy parameter on diffuse reflection of light, *Optics Communications*, pp:18-22.
2. R. F. Bonner, R. Nossal, S. Havlin, and G. H. Weiss. **1987**. Model for photon migration in turbid biological media, *Optical Society of America OSA*, 4(3), pp:423-432.
3. O. Katz, E. Small, Y. Guan, and Y. Silberberg. **2014**. Noninvasive nonlinear focusing and imaging through strongly scattering turbid layers, *Optical Society of America OSA*, 1(3), pp:170-174.
4. Y. Liu, P. Lai, C. Ma, X. Xu, A. A. Grabar, and L. V. Wang. **2015**. Optical focusing deep inside dynamic scattering media with near-infrared time-reversed ultrasonically encoded (true) light, *Nature Communications*, 6(5904), pp:1-9.

5. R. G. Medina, L. F. P´erez, M. Y´epez, F. Scheffold, M. N. Vesperinas, and J. J. S´aenz.**2012**.Negative scattering asymmetry parameter for dipolar particles: Unusual reduction of the transport mean free path and radiation pressure, *cond-mat.mtrl-sci*, 5(42), pp:1-5.
6. N. Naik, C. Barsi, A. Velten, and R Raskar.**2014**.Estimating wide-angle, spatially varying reflectance using time-resolved inversion of backscattered light, *Optical Society of America OSA*, 31(5), pp:957-963.
7. C. L. Hsieh, Y. Pu, R. Grange, G. Laporte, and D. Psaltis.**2010**.Imaging through turbid layers by scanning the phase conjugated second harmonic radiation from a nanoparticle, *Optical Society of America OSA*, 18(20723), pp:20723-20731.
8. S.C.W. Hyde, N.P. Barry, R. Jones, J.C. Dainty, P.M.W. French.**1996**.High resolution depth resolved imaging through scattering media using time resolved holography, *Optics Communications*, pp:111- 116.
9. X Yang, C. L. Hsieh, Y. Pu, and D. Psaltis.**2012**.Three-dimensional scanning microscopy through thin turbid media”, *Optical Society of America OSA*, 20(3), pp:2500-2506.
10. D. Akbulut, T. J. Huisman, E. G. van Putten, W. L. Vos, and A. P. Mosk.**2011**.Focusing light through random photonic media by binary amplitude modulation, *Optical Society of America OSA*, 19(5),pp:4017-4029.
11. I. M. Vellekoop and C. M. Aegerter. Focusing light through living tissue, *Proceedings of SPIE - The International Society for Optical Engineering*,7554(755430), pp:1-10.
12. Y. Guan, O. Katz, E. Small, J. Zhou, and Y. Silberberg.**2012**.Polarization control of multiply scattered light through random media by wavefront shaping, *Optics Letters*, 37(22), pp:4663-4665.
13. J. Tang, R. N. Germain, and M. Cui.**2012**.Superpenetration optical microscopy by iterative multiphoton adaptive compensation technique, *Proc. Natl. Acad. Sci. USA*, 109(22), pp:8434-8439.
14. O. Katz, E. Small, Y. Guan, and Y. Silberberg.**2012**.Looking around corners and through thin turbid layers in real time with scattered incoherent light, *Nature Photonics*, 1(3), pp:170-173.
15. S. H. Chang and A. Taflove.**2004**.Numerical study of light correlations in a random medium close to the Anderson localization threshold, *Optics Letters*, 29(9), pp:917-919.
16. D. Kim, J. Moon, M. Kim, T. D. Yang, J. Kim, E. Chung and W. Choi.**2014**.Pixelation-free and real-time endoscopic imaging through a fiber bundle, *Optics Letters*, 39(7), pp:1921-1924.
17. S. B. Colak, D. G. Papaioannou, G. W. Hooft, M. B. van der Mark, H. Schomberg, J. C. J. Paasschens, J. B. M. Melissen, and N. A. A. J. van Asten.**1997**.Tomographic image reconstruction from optical projections in light-diffusing media, *Applied Optics*, 36(1), pp:180-213.
18. P. Hariharan.**2002**.*Basics of holography*, Cambridge University Press, Cambridge University Press publishing, USA, New York.
19. D. S. Wiersma.**2013**.Disordered photonics, *Nature Photonics*, 7(22), pp:188-196.
20. P. P. J. Zupancic.**2013**.Dynamic Holography and Beamshaping using Digital Micromirror Devices, M.Sc. Thesis, Ludwig-Maximilians-Universitat Munchen.
21. T. Kozacki.**2011**.Holographic display with tilted spatial light modulator, *Optical Society of America*, 50(20), pp:3579- 3588.
22. G. Curatu.**2009**.Analysis and design of wide angle foveated optical systems, M.Sc. Thesis, College of Optics and Photonics, University of Central Florida Orlando, Florida.
23. A. Solodar, I. Klapp, I. Abdul halim.**2014**.Annular liquid crystal spatial light modulator for beam shaping and extended depth of focus, *OpticsCommunications*,323, pp:167-173.
24. D. P. Sprunken.**2008**.A 2-D spatial light modulator for spatio-temporal shaping, M.Sc. Thesis of science, university of Twente, Enschede- the Netherlands.
25. J. Harriman, S. Gauzab, S. Wub, D. Wickc and B. Bagwellc.**2006**.Transmissive spatial light modulators with high figure-ofmerit liquid crystals for foveated imaging applications, *Proc. SPIE*, 6135(61350), pp:1-13.
26. S. Reichelt, and N. Leister.**2013**.Computational hologram synthesis and representation on spatial light modulators for real-time 3D holographic imaging, *Journal of Physics*, pp:1-10.
27. G. D. Boreman and E. R. Raudenbush.**1988**.Modulation depth characteristics of a liquid crystal television spatial light modulator, *Applied Optics*, 27(14), pp:2940-2943.

28. R.Pappu, B. Recht, J. Taylor, N. Gershenfeld. **2002**. Physical One-Way Functions, *Science*, 297, pp:2026- 2030.
29. M. J. Booth. **2014**. Adaptive optical microscopy: the ongoing quest for a perfect image, *Light: Science and Applications*, 3(165), pp:1-7.
30. I. M. Vellekoop, A. Lagendijk, and A. P. Mosk. **2010**. Exploiting disorder for perfect focusing, *Nature Photonics*, 4(320), pp:1-3.
31. Vellekoop, I. M. and Mosk, A. P. **2007**. Focusing coherent light through opaque strongly scattering media. *Optics Letter*, 32, pp:2309–2311.
32. A. Garpebring. **2006**. Adaptive Camera Optics Based on a Liquid Crystal Spatial Light Modulator, M.Sc. Thesis, Lulea University of Technology, Sweden.